Nationaal Lucht- en Ruimtevaartlaboratorium

National Aerospace Laboratory NLR

NLR-TP-2013-444

Computational ship airwake determination to support helicopter-ship dynamic interface assessment

J. van Muijden, O.J. Boelens, J. van der Vorst and J.H.M. Gooden

Nationaal Lucht- en Ruimtevaartlaboratorium
National Aerospace Laboratory NLR

Anthony Fokkerweg 2
P.O. Box 90502
1006 BM Amsterdam
The Netherlands
Telephone +31 (0)88 511 31 13
Fax +31 (0)88 511 32 10
www.nlr.nl

Nationaal Lucht- en Ruimtevaartlaboratorium
National Aerospace Laboratory NLR

Executive summary

Computational ship airwake determination to support helicopter-ship dynamic interface assessment

Problem area
Operating helicopters in a maritime environment boosts risks and pilot work load to higher levels than normally encountered during land-based operations. At the end of a long mission, landing the helicopter on a small moving platform in the turbulent environment behind a ship's superstructure under low visibility conditions is a significant challenge. Ship-helicopter operational limits (SHOL) define the limits of the conditions under which it is possible to perform safe take-offs and landings aboard a ship. These limits are unique for every possible combination of type of helicopter and type of ship. Assessment of SHOL requires a dedicated qualification programme.

In order to limit the necessary manpower, time and costs of a dedicated qualification programme, simulation has been investigated as a means to support the establishment of SHOL. In a flight simulator for the helicopter-ship environment, indications of operational limits can be obtained without risking the loss of equipment and personnel. For this purpose, the flight simulator should contain ship airwake data tables of sufficient quality and accuracy to realistically mimic the approach of the helicopter towards the ship for a sufficiently dense number of wind directions.

This report describes the outcome of the investigation into reliable and practical computational approaches for ship airwake determination.

Report no.
NLR-TP-2013-444

Author(s)
J. van Muijden
O.J. Boelens
J. van der Vorst
J.H.M. Gooden

Report classification
UNCLASSIFIED

Date
October 2013

Knowledge area(s)
Computational Physics en theoretische aërodynamica
Helikoptertechnologie

Descriptor(s)
CFD-capability
ship airwake
wind climate
helicopter-ship simulation
SHOL

This report is based on a presentation held at the 21st AIAA Computational Fluid Dynamics conference, San Diego, U.S.A., June 24-27, 2013.

Also, an approach is described to implement the computed airwake into the helicopter flight simulator in a practical fashion. Thus, pilots have been enabled to fly through computed airwakes and to reflect on the reliability looks-and-feel of the various computational approaches.

Description of work

A CFD-capability has been developed to support the determination of SHOL. The airwake computation is based on fully viscous modelling. For the bulk of data, a steady Reynolds-averaged Navier-Stokes (RANS) approach is used for efficiency reasons. For more detailed flow data at specific conditions as well as for scientific research into higher physical levels of flow modelling, a hybrid Navier-Stokes/Large-Eddy Simulation (hybrid RANS-LES) approach has been applied.

Furthermore, a procedure to convert the computed airwake data into a suitable format for the helicopter flight simulator has been devised and tested.

Results and conclusions

It is shown that RANS-results are capable of indicating trends in flow vectors and local flow directions, although a deviation is usually observed with experimental results. The deviation in velocity ratio with respect to the experimental data in the present paper amounts to about 0.2 for RANS-based simulations. It has been observed that results based on the hybrid RANS-LES approach are in general closer to the experimental data, having a deviation in velocity ratio in the order of 0.1with respect to the experimental results. Surprisingly, the higher physical level of flow modeling does not resolve all of the differences between the hybrid computational approach and experiment. Further investigation is needed to identify the origin of the remaining differences with experiment. It is currently not clear whether mesh refinement, a larger number of samples for averaged results, or perhaps a higher accuracy in the experiment is of influence on this comparison.

Also, the overall look-and-feel of hybrid RANS-LES based flow fields is tested alongside RANS-based flow fields in the helicopter flight simulator. Feedback from experienced pilots has been obtained on the reality level of simulated flow fields using the current data conversion procedure. The reality level of both RANS and hybrid RANS-LES approaches for the airwake are rated acceptable.

Applicability

The recommended CFD-techniques, of which results are shown in this report, are applicable to establish airwakes around naval vessels as well as other landing environments. Also, the transfer of computed airwake data into a suitable format for the helicopter flight simulator is directly available, allowing actual flight simulations to be performed at helicopter landing sites based on existing or planned ships and/or buildings.

Nationaal Lucht- en Ruimtevaartlaboratorium, National Aerospace Laboratory NLR

Anthony Fokkerweg 2, 1059 CM Amsterdam,
P.O. Box 90502, 1006 BM Amsterdam, The Netherlands
Telephone +31 88 511 31 13, Fax +31 88 511 32 10, Web site: www.nlr.nl

Nationaal Lucht- en Ruimtevaartlaboratorium
National Aerospace Laboratory NLR

NLR-TP-2013-444

Computational ship airwake determination to support helicopter-ship dynamic interface assessment

J. van Muijden, O.J. Boelens, J. van der Vorst and J.H.M. Gooden

This report is based on a presentation held at the 21st AIAA Computational Fluid Dynamics Conference, San Diego, U.S.A., June 24-27, 2013.

Customer	National Aerospace Laboratory NLR
Contract number	- - -
Owner	NLR
Division NLR	Aerospace Vehicles
Distribution	Unlimited
Classification of title	Unclassified
	October 2013

Approved by:

Author	Reviewer	Managing department
J. van Muijden	J. van der Vorst	K.M.J. de Cock
Date: 9-10-2013	Date: 11-10-2013	Date: 11/10/2013

Contents

Computational ship airwake determination to support helicopter-ship dynamic interface assessment

Jaap van Muijden[1], Okko J. Boelens[2], Jasper van der Vorst[3] and Joop H.M. Gooden[4]
National Aerospace Laboratory NLR, Amsterdam, The Netherlands

A highly important aspect of safe sea-based helicopter operation is the establishment of ship-helicopter operational limits for current and future helicopter/ship combinations. The capabilities of Computational Fluid Dynamics for the determination of ship airwakes have been investigated, aiming at complementing existing experimental data acquisition techniques consisting of wind tunnel and on-board full-scale measurements. In this paper, computed airwakes based on the Reynolds-averaged Navier-Stokes (RANS) equations as well as on a hybrid RANS-Large Eddy Simulation (LES) approach are compared with experimental data. The resulting airwakes have been converted for usage in a helicopter flight simulator to enable additional feed-back on the reality level of the computational approaches from experienced pilots. It is shown that, from a practical point of view, a useful first impression of the average flow characteristics in the ship airwake can be obtained from steady RANS flow modeling, although the more computationally intensive hybrid RANS-LES approach has an inherently better potential for capturing all of the physical content of the fluctuating flow fields.

Nomenclature

C_v	=	ratio of local velocity to free-stream velocity, defined as $(u^2 + v^2 + w^2)^{0.5}$
h	=	characteristic mesh cell size
k	=	turbulent kinetic energy
L	=	reference length of the ship
t	=	physical time
t^*	=	non-dimensional time, in CTS units
u	=	velocity component in x-direction, scaled with U
U	=	reference velocity of the free-stream flow
v	=	velocity component in y-direction, scaled with U
w	=	velocity component in z-direction, scaled with U
x, y, z	=	orthogonal Cartesian coordinate directions
β	=	sideslip angle of reference flow vector
β_{local}	=	local sideslip angle
Δt	=	time step
Δt^*	=	non-dimensional time step
ϕ	=	vertical deviation of local flow vector from the horizontal plane
χ	=	horizontal deviation of local flow vector from the oncoming flow direction, $\beta_{local} - \beta$
ω	=	specific turbulent dissipation rate
CFD	=	Computational Fluid Dynamics
CFL	=	Courant-Friedrichs-Lewy number, stability criterion for numerical integration
CTS	=	Convective Time Scale, defined as L/U, average time required for a fluid particle to pass the ship

[1] Senior Scientist, Department of Flight Physics and Loads, P.O.Box 90502, 1006 BM, Amsterdam, The Netherlands, AIAA Member.
[2] R&D Engineer, Department of Flight Physics and Loads, P.O.Box 90502, 1006 BM, Amsterdam, The Netherlands.
[3] Senior R&D Engineer, Department of Helicopters and Aeroacoustics, P.O. Box 90502, 1006 BM, Amsterdam, The Netherlands.
[4] Senior Scientist, Department of Helicopters and Aeroacoustics, P.O. Box 90502, 1006 BM, Amsterdam, The Netherlands.

DNW = German-Dutch Wind Tunnels
EARSM = Explicit Algebraic Reynolds Stress Model
LES = Large-Eddy Simulation
LPD = Landing Platform Dock
LST = Low-Speed Wind Tunnel
NLR = National Aerospace Laboratory, The Netherlands
PIV = Particle Image Velocimetry
POD = Proper Orthogonal Decomposition
RANS = Reynolds-Averaged Navier-Stokes
RNLN = Royal Netherlands Navy
SFSN = Simple Frigate Shape with NLR-devised bow
SHOL = Ship-Helicopter Operational Limits
TNT = Turbulent/Non-Turbulent
XLES = eXtra-Large Eddy Simulation, NLR's version of hybrid RANS-LES

I. Introduction

OPERATING helicopters in a maritime environment boosts risks and pilot work load to higher levels than normally encountered during land-based operations. At the end of a long mission, landing the helicopter on a small, moving platform in the turbulent environment behind a ship's superstructure under low visibility conditions is a significant challenge. Ship-Helicopter Operational Limits (SHOL) define the limits of the conditions under which it is possible to perform safe take-offs and landings aboard a ship. These limits are unique for every possible combination of type of helicopter and type of ship. Assessment of SHOL requires a dedicated qualification programme. In order to limit the necessary manpower, time and costs of a dedicated qualification programme, simulation has been investigated as a means to support the establishment of SHOL. In a helicopter pilot station simulating the helicopter-ship environment, indications of operational limits can be obtained without risking the loss of equipment and personnel. For this purpose, the helicopter pilot station should contain ship airwake data of sufficient quality and accuracy to realistically mimic the approach of the helicopter towards the ship for a sufficiently dense number of wind directions.

This paper describes the outcome of the investigation into reliable and practical computational approaches for ship airwake determination. The main objective has been to develop a computational capability to support the current method of determining SHOL for the Royal Netherlands Navy (RNLN) in the future through the use of piloted simulation. The study has focused on obtaining the ship's airwake in an efficient way by CFD. Both RANS and hybrid RANS-LES approaches have been applied. Validation of the computational approach has been based on direct comparison with experimental data obtained in the DNW-LST low-speed wind tunnel around generic frigate and real landing platform dock models. Subsequently, the computed airwake data have been converted into a suitable input data format for the helicopter pilot station to allow the use of the computed flow fields in preliminary SHOL-assessments by piloted simulation. In this way, difficult operational conditions or grey areas in the preliminary SHOL can be pinpointed prior to the actual sea trials. The resulting operational time at sea for SHOL-determination is expected to be reduced significantly. The focus in this paper is on the CFD-approach for airwake determination.

II. Background

The ship airwake environment poses a significant risk to flight operations with helicopters due to the generally unsteady nature of the airwake and the significant variations of downwash and upwash experienced by the helicopter due to vortices and dead-air regions behind the vessel's superstructure[1,2,5,6,9,10,13]. Characterization of the ship airwake environment for safer aircraft launch and recovery is therefore a vivid area in international research, as are the operational and simulation aspects of helicopters flying in the airwakes of ships.

It is becoming common practice to support the determination of ship-helicopter operational limits with computed airwakes. The advantage of computed airwakes over experimental data is found in the availability of the full flow field at once, whereas detailed experimental data are in most cases limited to certain regions above the flight deck and next to the ship. These experimental data are extremely relevant to capture the main unsteady features of the airwakes and to validate the CFD-approaches, but are less amenable for conversion to a helicopter pilot station.

With common present day computer capacity, the computational effort for the determination of full viscous flow fields around ships is moderate for RANS-based flow simulations. The RANS-approach uses a turbulence model to mimic the influences of fluctuating flow quantities on the averaged flow field. For more physically relevant time-

accurate data, a hybrid approach between the Reynolds-averaged Navier-Stokes formulation near solid walls and Large-Eddy Simulation away from solid walls (hybrid RANS-LES) is coming within reach[8]. The hybrid RANS-LES approach is less dependent on the turbulence model since the larger resolved vortices (large eddies) in the mesh are computed directly in a time-accurate way.

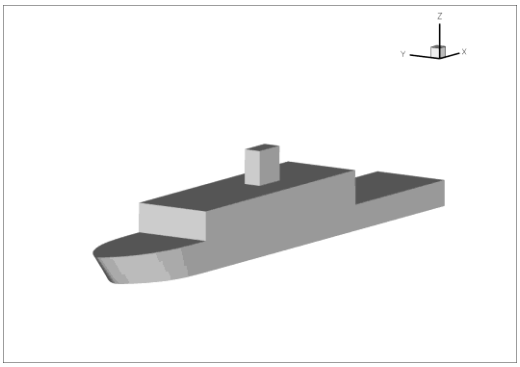

Figure 1. Geometry of SFSN, a simple frigate shape with NLR bow.

In the present paper, use has been made of steady RANS-simulations to obtain the bulk of the airwake data and on hybrid RANS-LES simulations to identify the needs for more physically relevant airwake data.

III. CFD-based airwake determination

A. CFD-method and meshes

For the fluid flow simulations, use has been made of the NLR in-house developed CFD-system ENFLOW, based on the solution of conservation laws on multi-block structured meshes[8]. ENFLOW allows the user to specify the flow model for a specific computational application, ranging from Euler (inviscid), RANS and hybrid RANS-LES flow models. In the latter two cases, a turbulence model is needed to specify the impact of turbulent fluid motion on the non-resolved spatial and temporal scales. In the case of RANS-simulations, the turbulence model is required in all boundary layers and in the shear layers shed from the configuration. In the case of hybrid RANS-LES, the role of the turbulence model is limited to boundary layers. A subgrid scale model is used in the other parts of the flow field. Switching between RANS and LES-regions is automatically determined depending on the RANS mixing length scale and the LES filter width. The NLR-version of hybrid RANS-LES including the automatic switching between regions is called X-LES (eXtra Large Eddy Simulation).

Figure 2. Landing Platform Dock LPD-2 'Johan de Witt'.

The main turbulence model in ENFLOW is the TNT k-ω model[7]. For improved realism in turbulence modeling for many applications, the enhancement with an Explicit Algebraic Reynolds Stress Model (EARSM) is an available option[12]. The computational results in this paper are performed using the k-ω model with the EARSM enhancement.

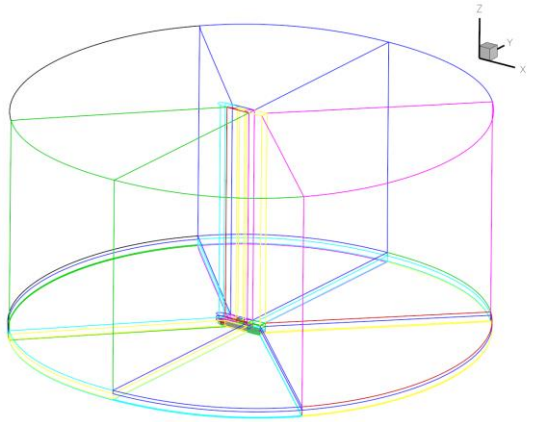

Figure 3. Shape of the far-field boundaries of the computational domain of SFSN.

For time-accurate hybrid RANS-LES simulations, experience from the past has led to a number of improvements to increase the practical applicability of the hybrid approach to realistic fluid flow problems. The improvements consist of:

- implementation of a fourth order accurate spatial scheme[8];
- addition of stochastic disturbances in the sub-grid scale model to improve the onset of unsteady motion in the LES-regions;
- significant reduction of the higher-order artificial dissipation terms to lower the dissipative characteristics of the flow model relative to the RANS-approach.

The second improvement is needed to overcome the inherent stability in viscous fluid flow simulations, where the far-field inflow conditions and

boundary conditions are way too constant and stable to represent the actual atmospheric boundary conditions in real situations.

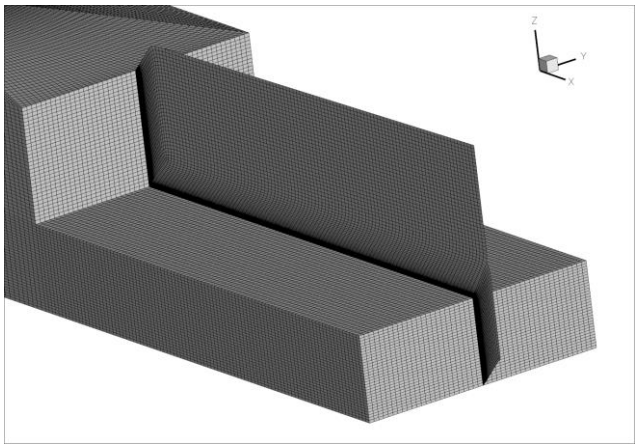

Figure 4. Details of mesh on the flight deck of SFSN.

Two configurations have been used for the assessment of the current state-of-the-art in this paper, using a simple frigate shape with a realistic bow as devised by NLR (SFSN, see Figure 1) and a realistic Landing Platform Dock (LPD-2, see Figure 2) in use by the RNLN. Other variants of the SFS have been investigated as wel; the experimental dataset for these alternative configurations is however less exhaustive. These variants are not reproduced in this paper. An impression of the type of mesh used in the current study is shown in Figure 3. To closely follow the characteristics of the wind tunnel experiments, the far-field distance in the computational mesh has been tuned in such a way that the tunnel floor boundary layer thickness matches the experimental value near the ship. To have similar performance for each flow direction, the far-field of the computational domain has been given a circular shape, thus assuring the same tunnel floor boundary layer for each flow angle.

The mesh for the SFSN consists of 58 blocks and 15.9 million cells. One mesh plane on the flight deck as well as the surface mesh are shown in Figure 4. The LPD-2 mesh is more complex due to the larger number of details on the ship (see Figure 5). Some of these details have already been left out or modified in the geometry as used for meshing. The geometry as applied in the mesh is shown in Figure 6. The final mesh for LPD-2 contains 33.1 million cells in 5746 blocks. The large difference in number of blocks is partially due to the manual topology generation for the SFSN as opposed to the semi-automatic topology generation for the LPD-2. An impression of the multi-block topology near the ship is shown in Figure 7.

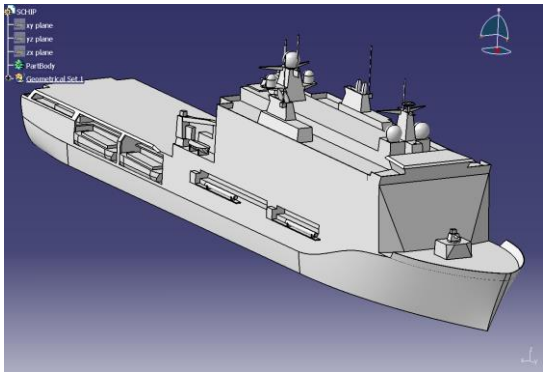

Figure 5. CAD-model of LPD-2.

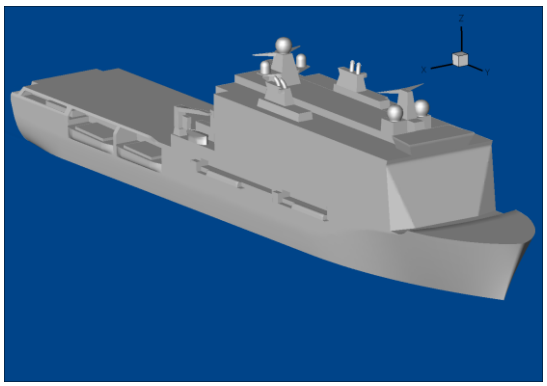

Figure 6. Geometry of LPD-2 as applied in the computational mesh.

B. Specific considerations for hybrid RANS-LES computations

Some considerations for practical applications of hybrid RANS-LES simulations have to be addressed. The efficient application of the hybrid RANS-LES approach strongly depends on the availability of computer power. Feasible mesh densities and the associated problem turn-around times are directly linked to the available computer power. Establishing the simulation parameters of hybrid RANS-LES computations are based on the following considerations:

- balancing spatial and temporal accuracy;
- statistical convergence of the mean flow;
- sampling frequency of the unsteady flow field;
- practical considerations related to affordable cost and allowable turn-around times.

The final choice of simulation parameters depends on the outcome of all of these considerations and the main focus of the simulation.

1. Balancing spatial and temporal accuracy

The scale of the ship and the velocity of the flow determine the convective time scale (CTS). The CTS can be defined as the approximate time it takes for a fluid particle to pass along the ship. For the simple frigate shapes, having a wind tunnel model reference length L of 1.28 m and a velocity U of 30 m/s, one CTS equals 0.043 s of

physical time. The determination of an appropriate time step for the simulations is derived as follows. At first, the spatial mesh resolution has to be adjusted to allow for a sufficiently dense and near-uniform mesh in the regions behind the ship's superstructure where large recirculation bubbles in the flow are expected. The spatial mesh forms the basis for the derivation of the time step by balancing the accuracy in spatial and temporal terms. Let us assume that a smallest mesh cell dimension *h* is present in the mesh. Current practice, based on second-order time integration and fourth-order spatial discretization, implies that a local CFL-number of about 1/8 is needed for equal accuracy in space and time. Translated into an estimate for the physical time step, this yields a time step of $\Delta t = h*CFL/U$. Expressed in terms of scaled or non-dimentional time as used by the flow solver (with units CTS), this results in a scaled time step of magnitude $\Delta t^* = h/(8*L)$. For the SFSN, having about 176 cells in streamwise direction, an appropriate scaled time step of 0.0007 is obtained.

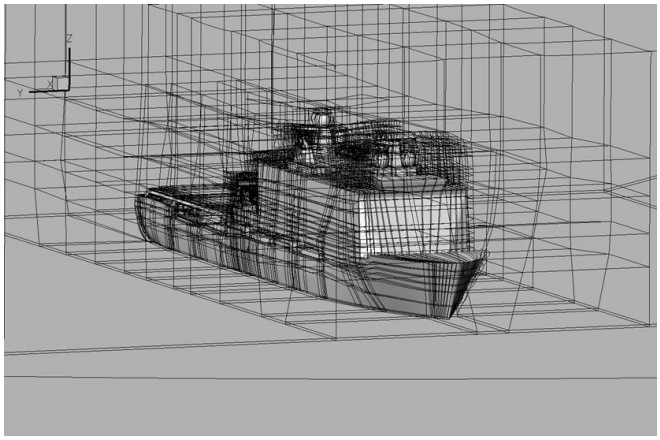

Figure 7. Impression of semi-automatically generated multi-block mesh topology around LPD-2.

2. Statistical convergence of the mean flow

Another way of looking at hybrid RANS-LES simulations is by addressing the statistical convergence of the mean flow field, see e.g. appendix B of Ref. 4. A very good convergence of the mean flow field (i.e. 5 percent uncertainty) requires 165 statistically independent samples, while a convergence with 10 percent uncertainty requires 41 statistically independent samples. Since instantaneous flow solutions at subsequent time steps are not statistically independent, a sufficiently large number of time steps has to be taken in between samples, e.g. 50 to 100. Thus, a sufficiently long simulation time in order to arrive at those independent samples amounts easily to at least 8 CTS, or even significantly more when higher accuracy in the mean flow is required.

3. Sampling frequency of the unsteady flow field

For the simulation of the unsteady flow field, the sampling frequency of the unsteadiness has to contain the range of interest of relevant frequencies for the application at hand. For helicopter landings on frigates, the full-scale frequency range of interest capable to affect helicopter motion is between 0.2 and 2 Hz. For a 1/60-scale model of SFSN and taking into account a factor 2 in free-stream velocity difference between full-scale ship and wind tunnel, this corresponds in the wind tunnel to a frequency range of 24-240 Hz. Sampling this frequency range will be adequate with a sampling rate of about double of the highest frequency, say 480 Hz. This implies that the unsteady flow field has to be stored at least 480 times per second, that is every 69^{th} time step (assuming the non-dimensional time step of 0.0007). This estimate also shows that there is room for enlargement of the time step for more practicality in the simulations.

4. Practical considerations related to cost and turn-around times

In the paragraph above on balancing the spatial and temporal accuracy, a time step of 0.0007 has been derived for hybrid RANS-LES flow simulations around the SFSN. However, from practical considerations, it is often preferred to have a nice rounded integer number of time steps per CTS, e.g. 1000. Thus, a scaled time step of 0.001 is more practical and still forms a good initial guess for the scaled time step. However, there are also turn-around time considerations for practical applications of the hybrid RANS-LES approach, especially when a large number of convective time scales are requested to study the long-term development of the unsteady flow and to obtain a high accuracy in the statistical convergence of the averaged mean flow field. Such simulations can take months of turn-around times if too much emphasis is placed on the time step. For such lengthy simulations, it seems overdone to perform 1000 time steps per convective time scale and a value of 500 time steps per CTS is still deemed appropriate (scaled time step of 0.002). In the latter case, the physical time step of the flow simulation is still less than 0.1 ms. With this time step, the sampling frequency of the unsteady flow field at a rate of 480 Hz requires storage of the flow field at least every 24^{th} time step. The number of time steps for simulating about 8 CTS amounts to 4000 after the initial transient state has been run. These values have been applied in the hybrid RANS-LES simulations. The averaged results have been obtained by sampling over 8.2 CTS or 0.3526 s of real time, with a stored flow solution at every 20^{th} time step.

C. Validation data

Validation of the computed airwake fields is done by comparison of results with experimental data[11]. The main purpose of the wind tunnel test campaign was to obtain time-averaged and unsteady flow field data around several ship models for CFD-validation and for use in the helicopter flight simulator. Due to the complicated flow field and the extended separations occurring behind the ship's superstructure, Particle Image Velocimetry (PIV) was selected as the primary measurement technique, especially for data collection in the flow recirculation regions as these regions cannot be measured by pressure probes or hot wires. PIV is particularly suited for the determination of the instantaneous flow field. However, measuring time-dependent turbulence data is not straight-forward using PIV due to the low data acquisition rate; this rate is in the current experiments about 2 Hz. This data acquisition rate is too low to obtain time-accurate velocity signals and associated spectra. The unsteady PIV data were therefore complemented with hot wire data at a few positions.

Figure 8. Wind tunnel model of the LPD-2 'Johan de Witt' in the DNW-LST wind tunnel.

The tests were performed in the Low Speed wind Tunnel (LST) of DNW. This is an atmospheric wind tunnel of the closed return type with a contraction ratio of 9. The maximum velocity in the empty test section is about 80 m/s. The test section has a cross-section of 3 m by 2.25 m. Two different ship models were tested in this tunnel: a model of the RNLN Landing Platform Dock 2 (LPD-2 'Johan de Witt', of which the wind tunnel model in the test section is shown in Figure 8) and a generic Simple Frigate Shape model (SFSN, see Figure 1) having a simple yet realistic bow shape as devised by NLR. Since ships are blunt bodies that render the results practically independent of Reynolds number, the velocity has been selected at 30 m/s which is an adequate velocity for PIV-measurements.

Three-component PIV data were acquired at different heights above the helicopter deck for various wind directions. Two cameras were mounted on the top turntable in the ceiling of the wind tunnel, assuring that the field of view relative to the ship remains unchanged under sideslip variations. The approach using two cameras results in a somewhat lower accuracy in velocity components in z-direction. The physical dimensions of the field of view were chosen to cover the most relevant part of the flight deck in one picture frame (field of view is about 0.4 m by 0.4 m). Also some data on the leeward and windward side of the upper structure have been obtained. At each data point 1024 flow samples have been taken, to enable analysis of the statistical turbulent flow properties. Besides PIV and hot wires also pressure probe measurements and flow visualization using smoke, oil and tufts were performed. In the comparisons shown in this paper, mainly the highly informative PIV-data have been used.

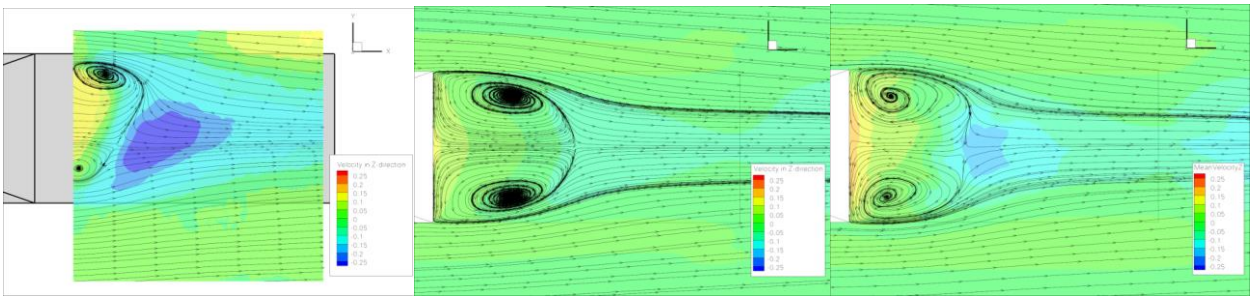

Figure 9. Comparison of experimental (left), RANS (middle) and hybrid RANS-LES results (right) for a plane at half-hangar height above the flight deck of the SFSN.

D. Global comparison of main flow features of SFSN at zero sideslip

A global impression of the experimental and computational results of the flow field for the SFSN at half-hangar height above the flight deck is shown in Figure 9. This condition is for a zero sideslip angle (straight head wind). Here, results are shown in a horizontal cross-plane at half-hangar height for the experiment, for a steady RANS-simulation, and for the averaged result of a hybrid RANS-LES flow simulation. In this plane, the velocity vector components are used to determine the topological signature of the flow by streamtraces, while the vertical velocity

component is given by the color scale of the picture. The red colour indicates a positive velocity in z-direction, the blue color indicates a negative velocity. It is shown that the averaged experimental data exhibit an asymmetrical solution. This asymmetry has been found in many other experiments on SFS-configurations. The steady RANS result is perfectly symmetrical, whereas the average of the hybrid RANS-LES simulation is nearly symmetrical. It is sometimes stated that the zero sideslip case for such a blunt object is the most difficult case, both for experiment and simulation, due to the sensitivity of the flow solution to minor deviations in parameters. Based on this and other planes of comparisons, it has been suggested that the stability of the shear layers coming from the sides of the superstructure still could be too stable in the hybrid RANS-LES simulations. Another observation is that the magnitude of the recirculating zone on the flight deck seems to be slightly overpredicted with steady RANS simulations. The magnitude of the recirculating zone obtained with the steady RANS model is subject to details of the turbulence model used.

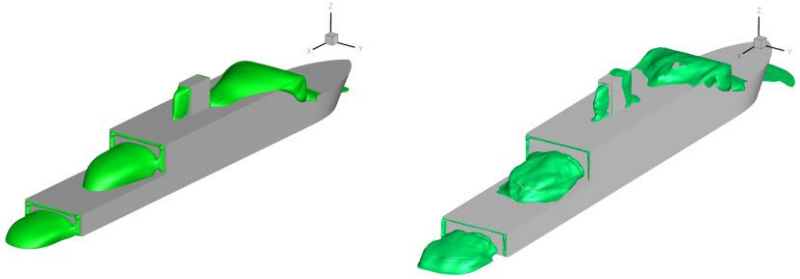

Figure 10. Comparison of the magnitude and shape of recirculation zones (zones with negative velocity in x-direction) in RANS (left) and averaged hybrid RANS-LES results (right).

Another global comparison of the main flow features is achieved by visualizing the zone with a negative velocity component in x-direction, see Figure 10. For the steady RANS simulation, this recirculation area is a massive zone starting from the shear layers leaving the sides of the superstructure. For the hybrid RANS-LES simulation, which is the result of averaging an inherently time-dependent flow, the result is less massive and prone to some randomness in shape. The visualization in this way again shows that the size of the recirculation zone on the flight deck is slightly smaller and of different shape than in the RANS-result.

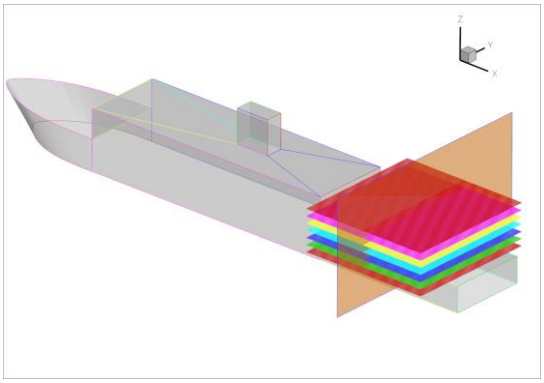

Figure 11. Seven horizontal PIV-planes above the flight deck of SFSN; the vertical plane indicates a mid-deck cut through the dataset.

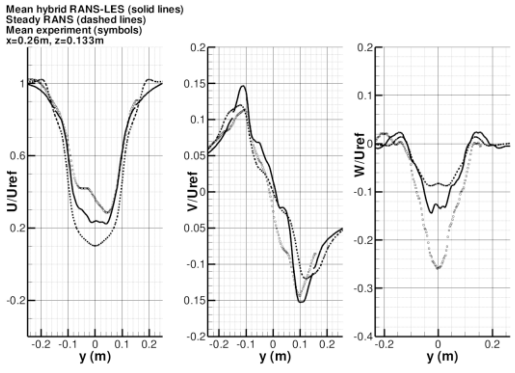

Figure 12. Direct comparison of scaled velocity components at half-hangar height above the landing spot.

E. Detailed comparison of results for SFSN at zero sideslip

Experimental data on the SFSN have been obtained in seven horizontal PIV-planes above the flight deck, see Figure 11. In terms of hangar height, these PIV-planes are located at 0.1, 0.3, 0.5, 0.7, 0.9, 1.1 and 1.3 hangar heights above deck. For a detailed comparison with the computational results, a number of cuts have been made through these PIV-planes to get information of velocity components in well-defined lines across the flight deck. Since reproducing the comparisons of results for all these lines is rather demanding and fills a complete report on its own, a severe subselection of results has been made at five equally distributed locations in x-direction on the helicopter deck in the plane at half-hangar height, and above the assumed helicopter landing spot at mid-deck (x=0.26 m, indicated by the vertical plane in Figure 11). Note that x=0 m refers to the hangar door position.

From the experiment as well as the computations of the flow field, velocity components in the three axis directions have been obtained. These components can be compared directly to obtain an impression of the performance of different CFD-approaches for flows including large recirculation zones. An example of comparing velocity components at half-hangar height above the landing spot is depicted in Figure 12. At first sight, the curves of computed

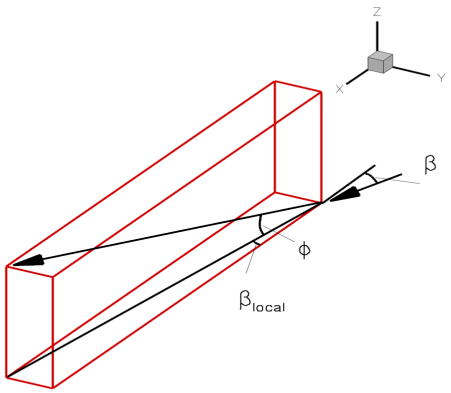

Figure 13. Clarification of the representation of the velocity vector as a velocity ratio and local flow deviation angles

results show similar behavior as the experimental data. The differences between RANS and hybrid RANS-LES results are indicative for the higher physical level of modeling of the latter approach; those results lie closer to the experimental data. Nevertheless, not all differences between hybrid RANS-LES and the experimental data are resolved. Since it is possible that deviations in one velocity component are compensated in another, it is a more common approach in SHOL-related airwake determination to write fluid flow field results in terms of the velocity ratio C_v, local horizontal deviation angle from the oncoming flow direction $\chi=\beta_{local}-\beta$, and local vertical deviation angle from the horizontal plane, ϕ. The definition of this way of representing the local velocity vector and local flow directions is further clarified in Figure 13. In the following, this representation of results will be used.

The results for zero sideslip at half-hangar height over the flight deck at five locations in x-direction (x=0.12, 0.19, 0.26, 0.33 and 0.40 m) are shown in Figure 14. The blue lines and symbols represent the velocity magnitude (the scale for velocity magnitude is found on the left-hand side of the pictures). The green and red lines and symbols represent the horizontal and vertical flow angle deviations (the scale for flow deviation angles is found on the right-hand side of the pictures).

Note that the picture on the left in the middle row of Figure 14 contains exactly the same data as Figure 12, this time however in the alternative data representation. The results in Figure 12 show a rather good agreement in the velocity in y-direction, with larger deviations in the other two velocity components. The hybrid RANS-LES results are similar in character as the RANS results, although a little better in comparison with the experiment. In the left picture in the middle row of Figure 14, the same information gives an additional view on the results. It is shown that the local flow angles are represented quite well with only minor deviations from the experimental results. There is, however, a remaining deviation in velocity ratio with experiment which is slightly smaller for the hybrid RANS-LES results.

It is observed from Figure 14 that, closest to the hangar door, the velocity ratio appears to have the right value over the entire range, however with deviations in the flow angles. For very small velocity vector magnitudes, however, the sensitivity of flow angles to small changes in velocity components is large. Note that, optically, large steps in horizontal flow angles of 360 degrees sometimes occur, but one should remember that a horizontal flow angle deviation of -180 degrees is identical to 180 degrees. When moving aft from hangar door to stern, the deviations in flow angles practically disappear, however with a remaining discrepancy in flow vector magnitude. Over the whole range, the hybrid RANS-LES results are closer to the experimental data than the RANS results. At present, the hybrid RANS-LES approach does not resolve all of the differences with the experimental data. This is partially due to the asymmetry in the experimental data that is not fully understood yet. However, also in flow regions sufficiently far outside of the recirculation zones the deviation in velocity ratio persists.

A further view on the dataset above deck is shown in the data cuts that are taken at mid-deck position for increasing heights above deck, see Figure 15. Note that the result at half-hangar height at this location is already included in Figure 14. Two observations are immediately clear. The first one is that deviations in local flow angles only occur in cuts below half-hangar height. At or above half-hangar height, the flow angles from computations and experiment are almost identical. Furthermore, even for the highest elevation above deck, the velocity ratio from the simulations is still significantly different from the experimental results, in the order of 0.2 for RANS-results and in the order of 0.1 for hybrid RANS-LES results. Even thought the hybrid RANS-LES results are closer to the experimental results, there is still no match at any height above deck. This is a somewhat surprising observation; one might expect that at a location sufficiently far away from the ship the experimental and computed results should converge, not only in terms of local flow angles but also in velocity ratio.

F. Detailed comparison of results for SFSN at 15 degrees sideslip

The comparison of results at half-hangar height for the SFSN at 15 degrees sideslip angle are shown in Figure 16. For this condition, only RANS-based computational results are available at present. It is observed in Figure 16 that

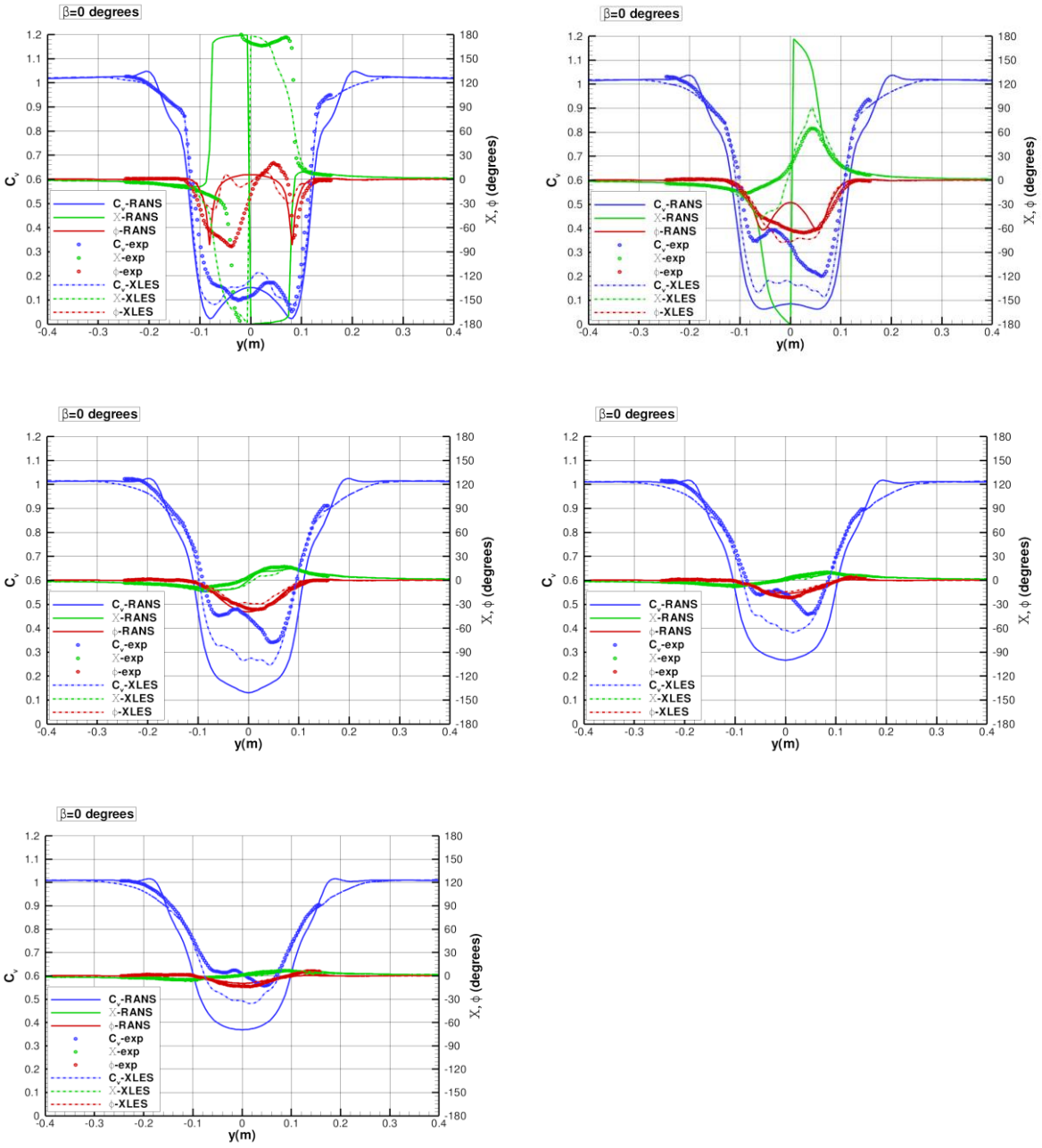

Figure 14. Comparison of computed and experimental results at half-hangar height for zero sideslip; top row from left to right x=0.12 and x=0.19 m, middle row x=0.26 and x=0.33 m, bottom row x=0.40 m.

the deviations in flow angles are in general moderate (apart from a few larger deviations at small velocity ratio) and improving when approaching the stern. The shape of the velocity ratio is rather well predicted for most of the data cuts. On the windward side of the deck for this sideslip angle, i.e. the right-hand side, the RANS-based CFD-results show a rather strong localized vortex all along the deck length whereas the experimental data show a more gradually decreasing vortex towards the stern. Although this trend is identical in the CFD-results, the comparison between computation and experiment for the velocity ratio starts out rather well at the right-hand side closest to the hangar door in Figure 16, while deviations become gradually larger towards the stern. On the leeward side, i.e. the left-hand side for this sideslip angle, the experimental data show a stronger vortex action in the velocity ratio distribution than the computational results. Here, too, the trends are similar between experiment and computations although the exact

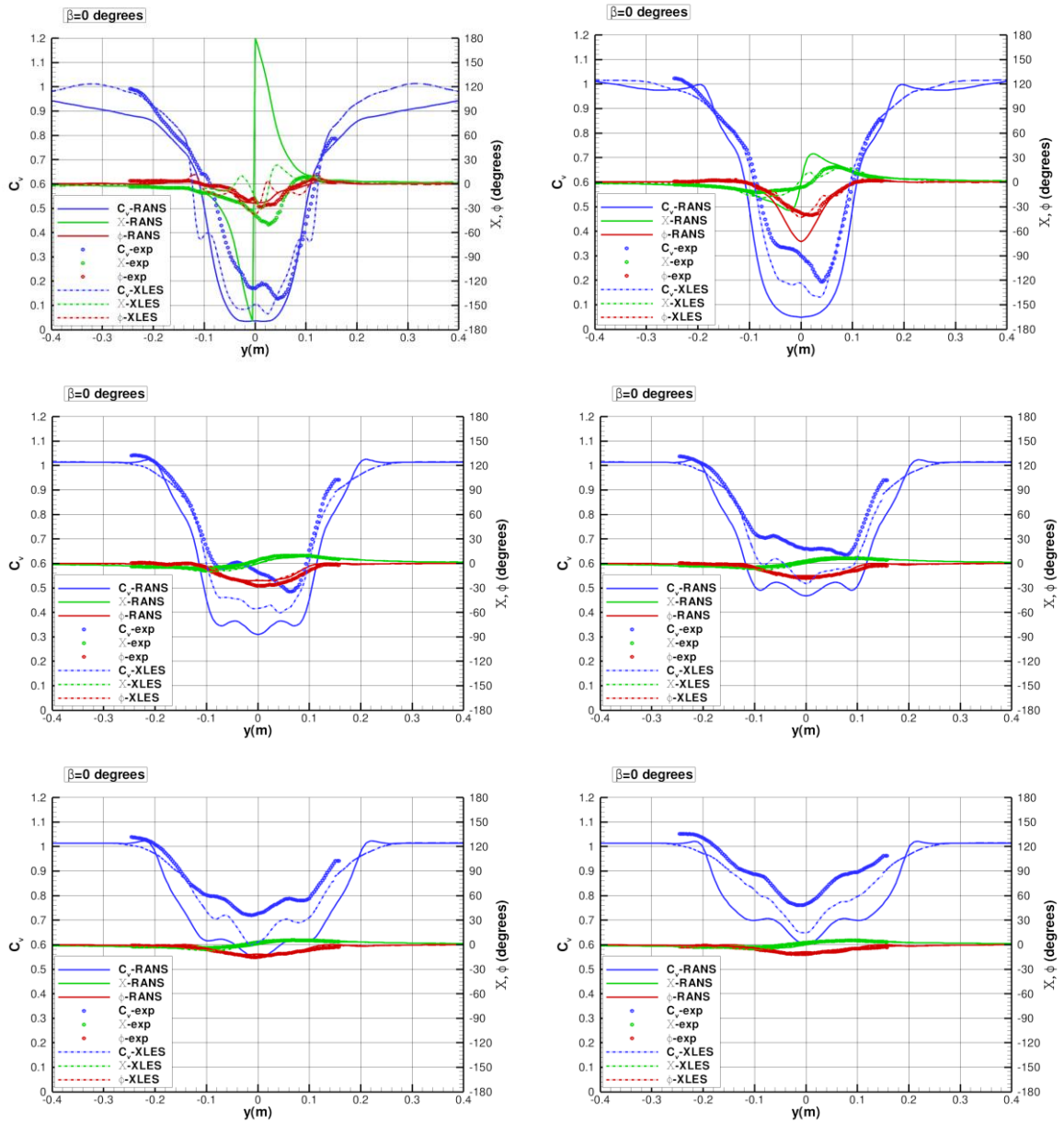

Figure 15. Comparison of computed and experimental results at mid-deck position for various heights above deck for zero sideslip; top row from left to right 0.1 and 0.3 hangar heights, middle row 0.7 and 0.9 hangar heights, bottom row 1.1 and 1.3 hangar heights. For result at 0.5 hangar height, see Figure 14, left picture in middle row.

location and magnitude of minimum and maximum velocity ratio differs. The order of deviation in the velocity ratio is about 0.2 as has been identified before for RANS-based results. The results for the mid-deck position at increasing height above deck at 15 degrees sideslip are depicted in Figure 17. Deviations in local flow angles are quite moderate and only locally present. The velocity ratio shows a too strong vortex action on the the windward side in the CFD-results. On the leeward side, the experimental velocity ratio shows a stronger variation as has also been noticed in the previous set of results. In general, the trends are recognizable from both the experimental and computational results. The order of magnitude of the persistent mismatch in velocity ratio is still of the order of about 0.2. Only the highest result above deck shows a diminishing difference in velocity ratio on the windward side. It can be expected that hybrid RANS-LES results are capable to reduce the currently observed differences with the

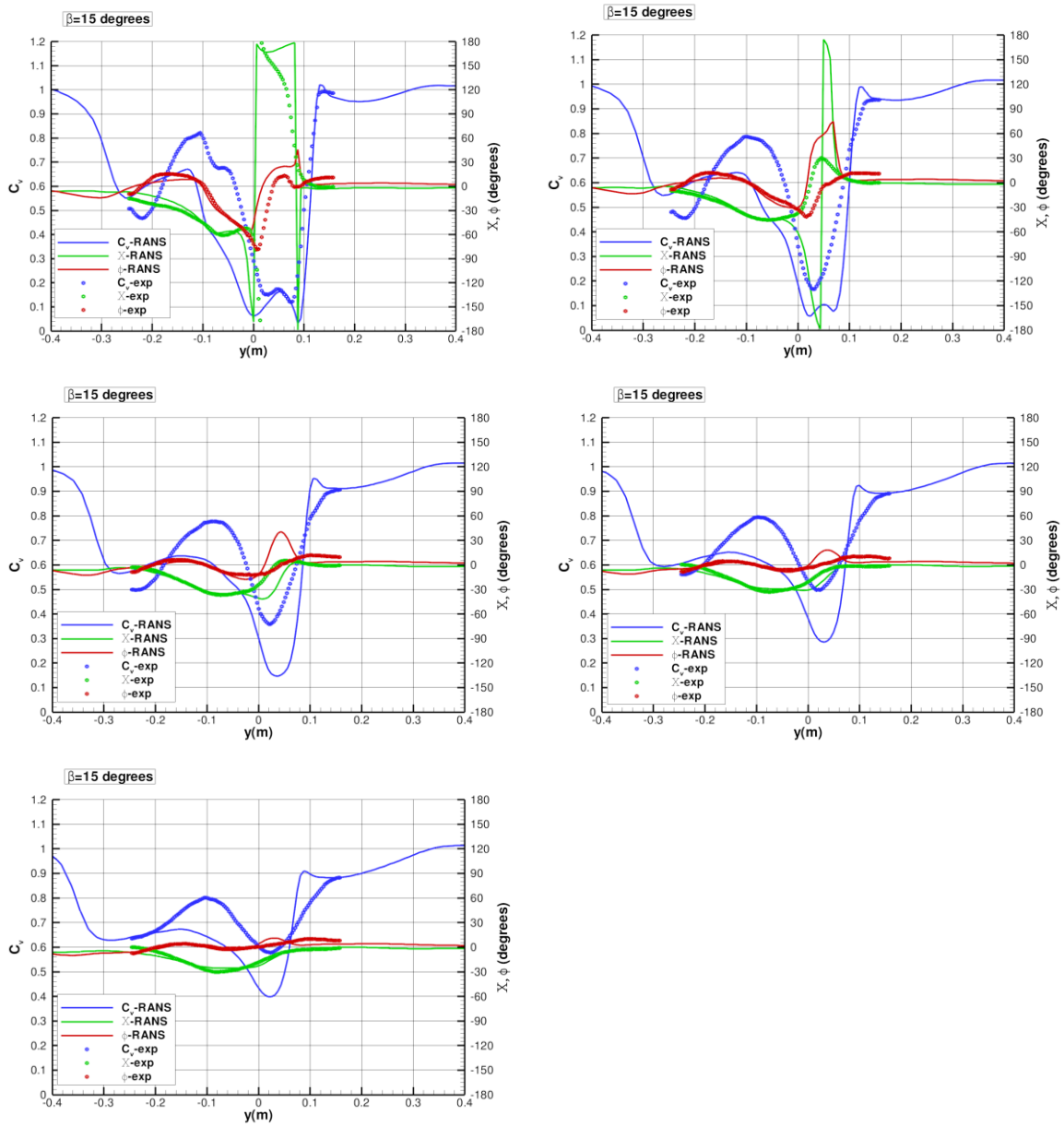

Figure 16. Comparison of computed and experimental results at half-hangar height for 15 degrees sideslip; top row from left to right x=0.12 and x=0.19 m, middle row x=0.26 and x=0.33 m, bottom row x=0.40 m.

experimental data, although it is unlikely that the full gap will be closed. This case seems rather complicated due to the interaction of deck edge vortices and shear layers from the superstructure, especially at the leeward side.

G. Detailed comparison of results for SFSN at 45 degrees sideslip

The final set of in-depth results to be shown here is obtained for the SFSN at 45 degrees sideslip angle. For this condition, only one PIV-plane has been measured at half-hangar height so there is no use in looking at other heights above deck. The five locations from hangar to stern at half-hangar height above deck are compared in Figure 18. This case appears to be less complicated in terms of interaction of deck edge vortices and shear layers from the superstructure. It is shown that local flow angles are reasonably well predicted with occasional larger deviations, and closer to the stern the deviations with experimental local flow angles practically vanish. Occasional larger deviations in local horizontal flow direction can be attributed to the difference in size of the recirculation zone, which is

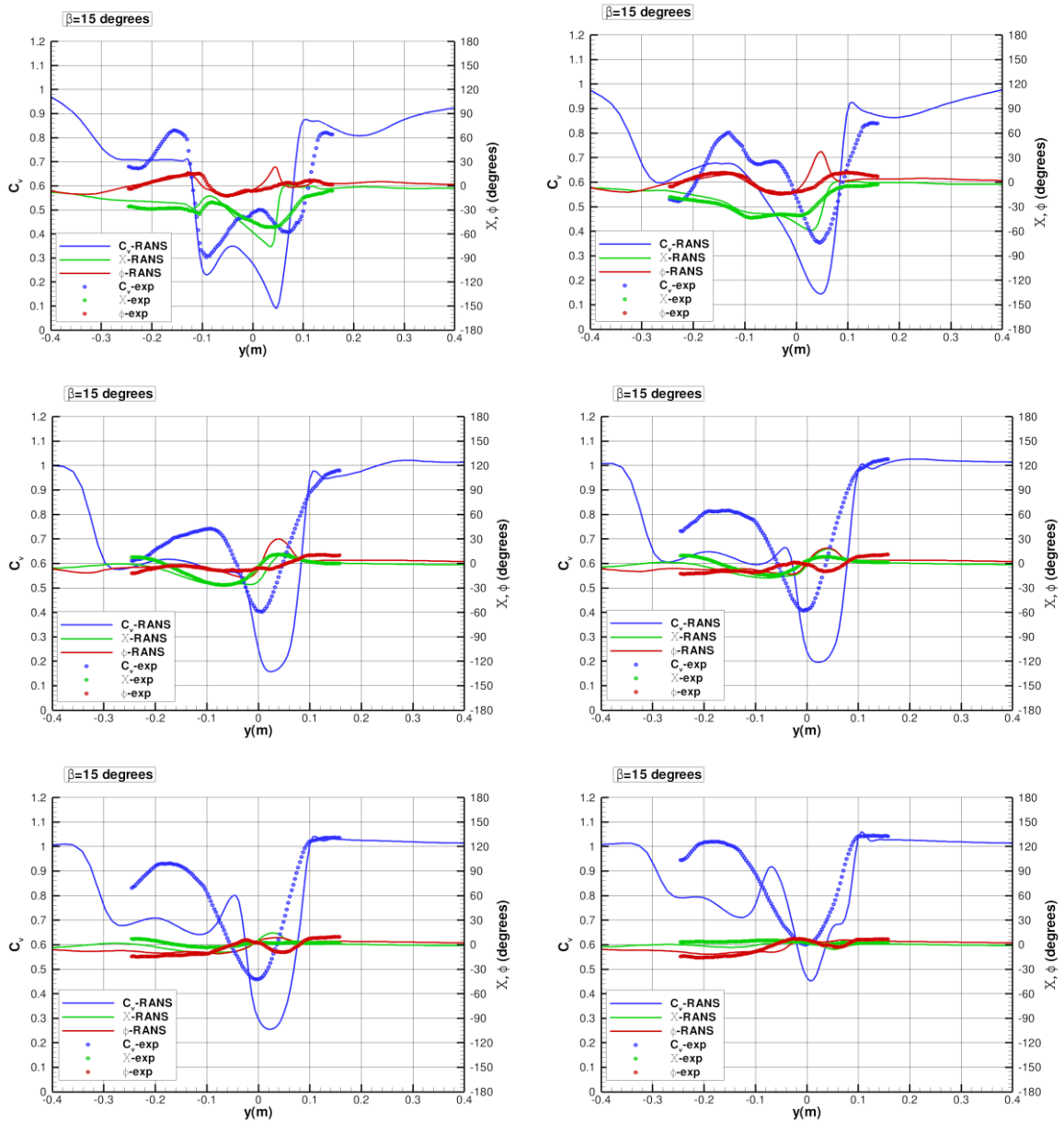

Figure 17. Comparison of computed and experimental results at mid-deck position for various heights above deck for 15 degrees sideslip; top row from left to right 0.1 and 0.3 hangar heights, middle row 0.7 and 0.9 hangar heights, bottom row 1.1 and 1.3 hangar heights. For result at 0.5 hangar height, see Figure 16, left picture in middle row.

generally too large in RANS-based results. For this particular sideslip angle, also the velocity ratio shows up quite good. The computed results of the velocity ratio follow the experimental results very adequately, showing that the location of vortices is well-defined and probably less sensitive to disturbances due to shear layers and vortices from the superstructure that are also quickly transported to the leeward side in this wind condition. Although the character of the velocity ratio is captured quite well in each of the cuts, there is still a remaining overshoot in magnitude. Being slightly smaller than in the other comparisons between RANS-results and experiment, the deviation in velocity ratio is in the order of 0.1-0.2. In the cut closest to the stern at a sideslip of 45 degrees, the influence of any upstream disturbance is expected to be absent, and indeed the best comparison between RANS and experimental results is found here.

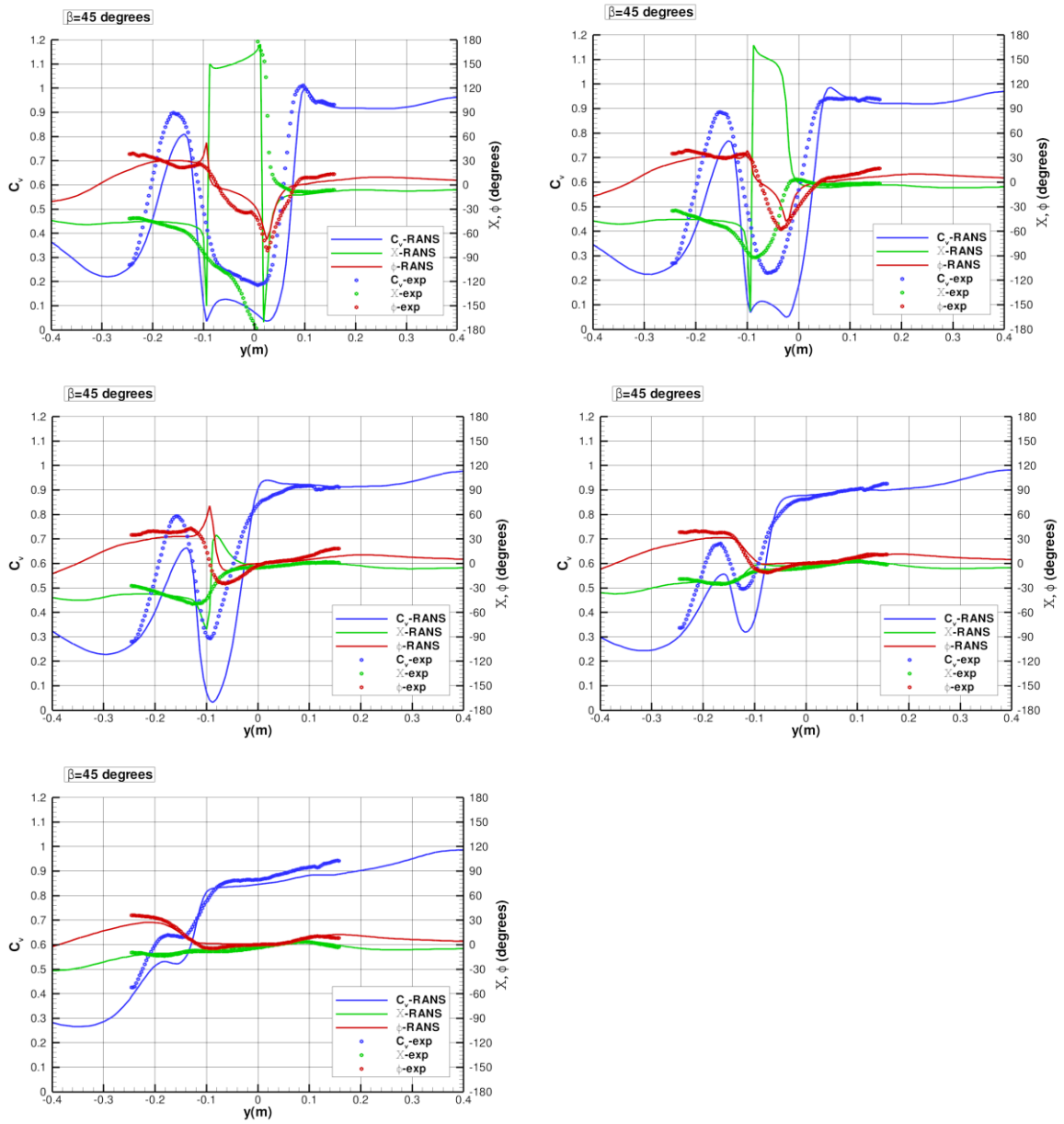

Figure 18. Comparison of computed and experimental results at half-hangar height for 45 degrees sideslip; top row from left to right x=0.12 and x=0.19 m, middle row x=0.26 and x=0.33 m, bottom row x=0.40 m.

Concluding, it has been shown that a RANS-based approach for the flow field on the helicopter deck of a ship is capable of determining trends in velocity magnitude and local flow angles, although one should not expect a perfect match due to the rather complex nature of mixing of deck-edge vortices and shear layers from the superstructure. Part of the deviations is due to the generally larger predicted recirculation zones in RANS-based simulations. A better result can be obtained by the physically more competent hybrid RANS-LES computations that take the unsteadiness of the flow field automatically into account. The hybrid RANS-LES approach delivers recirculation zones that are in better agreement with experimental data. However, it has also been observed that such a more advanced approach does not fully resolve the differences with experiment when looking at detailed flow vector data comparisons. Currently, the suitability of the presented CFD-approach is being investigated for preliminary SHOL-envelope predictions.

H. Global comparison of size of recirculation zones on LPD-2

The size of the recirculation zones has been found to vary with the computational method that one uses. In general, RANS-based computations deliver too large recirculation zones as compared to hybrid RANS-LES and experimental data. The differences for a generic frigate shape have been shown in the previous sections. Here, the impact of different computational approaches on recirculation zones on a realistic ship are investigated. Figure 19 shows a comparison of the impact of the computational method on the size and shape of recirculation zones. Again,

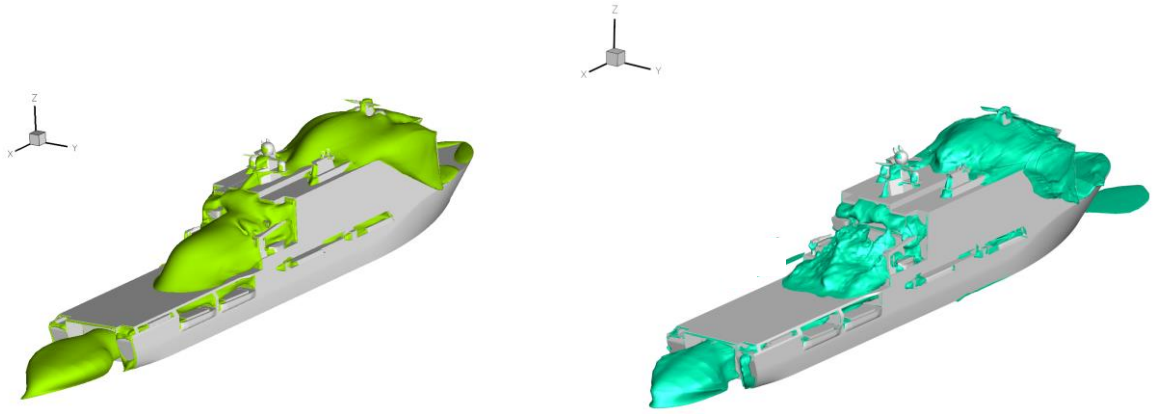

Figure 19. Differences in predicted recirculation zones on the LPD-2 at zero sideslip using RANS-based simulation (left) and hybrid RANS-LES based simulation (right).

it is found that the RANS-approach has the tendency to make the recirculation zones larger and also more voluminous than the hybrid RANS-LES approach. In this context, it can be remarked that some influence on the size and extent of the recirculation zones as predicted by RANS-methods can be exerted by varying the turbulence model.

IV. Conversion and usage of airwake data for helicopter pilot station

The computed data for each flow condition is obtained within the multitude of blocks as used for the meshing of the ships. For the helicopter pilot station, such a particular form of airwake data is too complex for real-time flight simulations and too large to fit into the available memory. A workable solution has been achieved by interpolating the data from the computed flow field into a single-block structured data field for usage in the helicopter pilot station[3]. In this interpolated block, shown in Figure 20, the spatial resolution is higher close to the ship and less dense at the edges of the block. The boundaries of the block have been selected at distances that are sufficiently far away to allow a smooth flight transition from the basically disturbance-free far field into the actual ship airwake. Interpolation of the dataset to the coordinates of the airwake block is performed within the flow visualization tool. The helicopter pilot station needs averaged velocity components as well as turbulence data (either from resolved fluctuating velocities or from the turbulence model) to be used in a filter for the generation of random fluctuations due to atmospheric disturbances. The sketched approach for data conversion from CFD-based flow solutions to a dataset

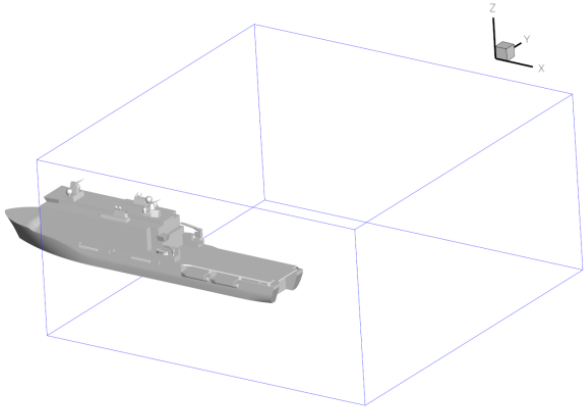

Figure 20. Data box around LPD-2 for data interpolation from simulated airwake for usage in the helicopter flight simulator

for the helicopter pilot station has been applied at NLR for the LPD-2 as well as for a hospital building in Amsterdam having an emergency helicopter platform on the roof[3]. The interesting part of this approach is that it is possible to have highly experienced pilots fly through the simulated airwake and deliver useful feedback on the realism of the simulated flow field. The reality level of both RANS and hybrid RANS-LES approaches for the airwake determination appears to be acceptable for experienced pilots. One can imagine, however, that flying through a simulated environment based on random turbulent motion as shown in Figure 21 is different from the less chaotic environment as shown in Figure 22. However, the actual simulator look-and-feel does not only depend on the type of airwake data used, but also on the way in which the dataset is converted.

Therefore, another approach for data conversion that might be of interest in the future for the helicopter pilot station is to reconstruct the time-accurate flow field from a POD-decomposition. In this approach, it is assumed that at each instant the time-dependent flow field can be decomposed into a finite set of steady flow field modes, multiplied by time-dependent coefficients. The flow field modes are obtained by a proper orthogonal decomposition of the computed time-dependent flow field. In this way, the helicopter pilot station needs to store a sufficient number of POD-modes together with the time-dependent coefficients. It depends on the memory requirements for one POD-mode and the available memory of the simulator what the limits of this reconstruction procedure will be.

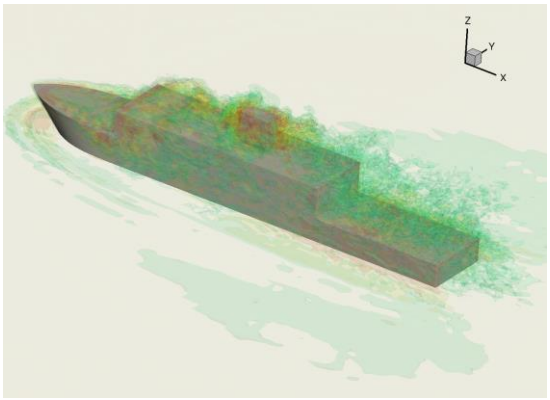

Figure 21. Three levels of vorticity in the air-wake of SFSN at zero sideslip; instantaneous view during hybrid RANS-LES simulations

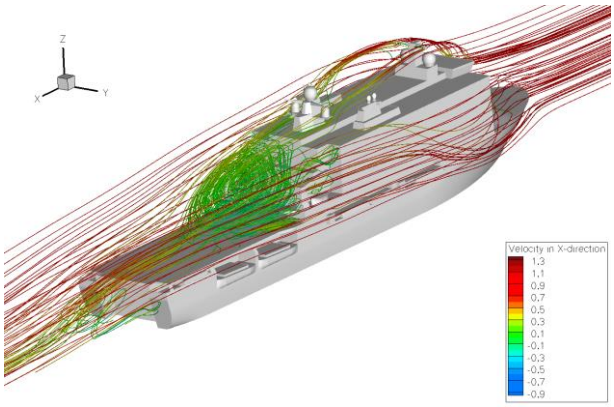

Figure 22. Streamlines over the superstructure of LPD-2 at zero sideslip; result of RANS simulation.

V. Conclusions

A CFD-capability has been developed to support the determination of SHOL. The airwake computation is based on fully viscous flow modeling. For the bulk of data, a steady RANS-approach is used for efficiency reasons. The RANS-results are capable of indicating trends in flow vectors and local flow directions, although a deviation is usually observed with experimental results. The deviation in velocity ratio, based on the experimental data in the present paper, amounts to about 0.2 for RANS-based simulations. For more detailed flow data at specific conditions as well as for scientific research into higher physical levels of flow modeling, a hybrid RANS-LES approach has been applied. It has been observed that results based on the hybrid RANS-LES approach are in general closer to the experimental data. The deviation in velocity ratio is in the order of 0.1 for hybrid RANS-LES results. Surprisingly, the higher physical level of flow modeling does not resolve all of the differences between the hybrid computational approach and experiment. Further investigation is needed to identify the origin of the remaining differences with experiment. It is currently not clear whether mesh refinement, a larger number of samples for averaged results, or perhaps a higher accuracy in the experiment is of influence on this comparison. Enhancements in turbulence modeling as well as in mesh resolution close to the shear layers shedding from the superstructure have been suggested for further improvements of simulated results. Despite deviations between simulated and experimental results, the trends and quality of simulated flow fields are sufficiently promising to investigate their possible applications in the determination of SHOL, even if only for a preliminary SHOL-envelope to pinpoint further detailed investigations.

Furthermore, a conversion procedure has been devised to convert computed flow field data (either based on RANS or on hybrid RANS-LES) into a data block for the helicopter flight simulator. This data transfer procedure is

based on data interpolation in the CFD-mesh to generate a single-block ordered data structure for the helicopter pilot station at a resolution that is sufficient for the helicopter motion simulations without the burden of storing the full CFD-dataset. Feedback from experienced pilots has been obtained on the reality level of simulated flow fields using the current data conversion procedure. The reality level of both RANS and hybrid RANS-LES approaches for the airwake determination is rated acceptable by experienced pilots.

Acknowledgments

The scientific research forming the basis for this paper has been partially funded by the Dutch Ministry of Defence through the National Technology Project "Rotorcraft-Ship Dynamic Interface Simulation (ROSDIS)-2" and partially by NLR's programmatic research "Kennis voor Beleid". Also, the support by Henk Haverdings of NLR in devising the data transfer procedure from the CFD-results to the helicopter pilot station data is gratefully recognized.

References

[1]Forrest, J.S., Hodge, S.J., Owen, I., and Padfield, G.D., "An investigation of ship airwake phenomena using time-accurate CFD and piloted helicopter flight simulation", *Proceedings of the 34th European Rotorcraft Forum*, 2008.

[2]Forrest, J.S., and Owen, I., "An investigation of ship airwakes using detached-eddy simulation", *Computers and Fluids*, Vol. 39, Nr. 4, pp. 656-673, 2010.

[3]Haverdings, H., "Helicopter emergency medical service (HEMS) from a rooftop in Amsterdam: a simulation perspective", *Proceedings of the 37th European Rotorcraft Forum*, paper 143, 2011, also NLR-TP-2012-586, 2012.

[4]Herry, B., "Etude aérodynamique d'une double marche descendante 3D appliquée a la sécurisation de l'appontage des hélicopters sur les frégates" , Ph.D. Thesis, Université de Valenciennes et du Hainaut Cambrésis, France, December 2010.

[5]Herry, B., Keirsbulck, L. Labraga, L., and Paquet, J.B., "Flow bistability downstream of three-dimensional double backward facing steps at zero-degree sideslip", *Journal of Fluids Engineering*, Vol. 133, Issue 5, May 2011.

[6]Herry, B., and Vorst, J. van der, "Towards the impact of flow bi-stability on the launch and recovery of helicopters on ships", AIAA-2011-7043, September 2011.

[7]Kok, J.C., "Resolving the dependence on freestream values for the k-omega turbulence model", *AIAA Journal*, Vol. 38, No. 7, pp. 1292-1294, July 2000.

[8]Kok, J.C., Soemarwoto, B.I., and Ven, H. van der, "Hybrid RANS-LES simulations at NLR using X-LES and a high-order finite-volume method", *DESider – A European effort on hybrid RANS-LES modeling*, edited by W. Haase, M. Braza, and A. Revell, Notes on Numerical Fluid Mechanics and Multidisciplinary Design, pp. 392-398, Vol. 103, Springer, 2009.

[9]Polsky, S.A., "A computational study of unsteady ship airwake", AIAA-2002-1022, 2002.

[10]Syms, G.F., "Simulation of simplified-frigate airwakes using a lattice-Boltzmann method", *Journal of Wind Engineering and Industrial Aerodynamics*, Vol. 96, pp. 1197-1206, 2008.

[11]Vorst, J. van der, Gooden, J., and Muijden, J. van, "Rotorcraft/ship dynamic interface simulation developments at NLR", *Proceedings of the 36th European Rotorcraft Forum*, 2010.

[12]Wallin, S., and Johansson, A.V., "An explicit algebraic Reynolds stress model for incompressible and compressible turbulent flows", *Journal of Fluid Mechanics*, Vol. 403, pp. 89-132, 2000.

[13]Zan, S.J., "On aerodynamic modeling and simulation of the dynamic interface", *Journal of Aerospace Engineering*, Vol. 219, Nr. 5, pp. 393-410, 2005.